



## Search for the Associated Chargino-Neutralino Production in the Final States with Two Muons and Additional Lepton

The DØ Collaboration  
URL: <http://www-d0.fnal.gov>  
(Dated: August 3, 2004)

A search for supersymmetry for the trilepton channel has been performed. A search for final states with two muons plus an additional lepton arising from the subsequent decay of the chargino  $\tilde{\chi}_1^\pm$  and the neutralino  $\tilde{\chi}_2^0$  has been performed with events collected by the DØ detector at the Fermilab Tevatron  $p\bar{p}$  collider at a center-of-mass energy of 1.96 TeV between August 2002 and March 2004. This data corresponds to an integrated luminosity of  $\mathcal{L} \approx 221 \text{ pb}^{-1}$ . We find one candidate passing our cuts, with expected background of  $1.83 \pm 0.40$  (stat.)  $\pm 0.21$  (syst.) events. This result provides input to a combined trilepton analysis.

*Preliminary Results for Summer 2004 Conferences*

## I. INTRODUCTION

An introduction to the theory of supersymmetry (SUSY) is given in [1]. This analysis is focused on the Minimal Supersymmetric Standard Model (MSSM): R-parity is conserved, supersymmetric particles are produced in pairs and the lightest supersymmetric particle (LSP)  $\tilde{\chi}_1^0$  is stable.

According to this model the higgsinos and electroweak gauginos mix with each other. The neutral higgsinos and neutral gauginos combine to form the four neutral mass eigenstates *neutralinos*  $\tilde{\chi}^0$  and the charged higgsinos and winos mix to form two charged mass eigenstates *charginos*  $\tilde{\chi}^\pm$ . The supersymmetric particles under investigation are produced as a  $\tilde{\chi}_1^\pm \tilde{\chi}_2^0$  pair and decay into leptons and the LSP. The final state is therefore characterized by leptons and a missing transverse energy from the  $\tilde{\chi}_1^0$  and the neutrino. A Feynman diagram for this decay is shown in Figure 1. The transverse momenta of the leptons in the final state depends on the masses of the neutralinos and charginos.

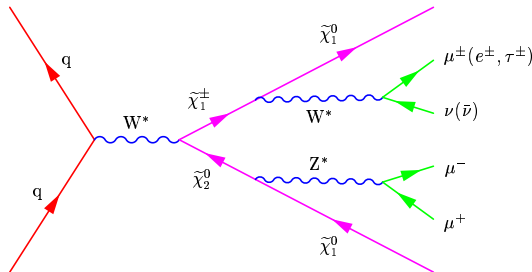


FIG. 1: Chargino-neutralino associated production in the final state with two muons:  $p\bar{p} \rightarrow \tilde{\chi}_1^\pm \tilde{\chi}_2^0 \rightarrow \ell\mu\nu\tilde{\chi}_1^0\tilde{\chi}_1^0$ . The diagram shows the dominant contribution for SUSY points where the slepton mass is larger than the gaugino mass.

## II. DØ DETECTOR

A detailed description of the DØ detector is given in [2]. Object of this analysis are reconstructed muons, whose tracks are detected by the muon system and the inner tracker. The muon system consists of a layer of tracking detectors and scintillating trigger counters before 1.8 T toroids, followed by two more similar layers after the toroids. Tracking at  $|\eta| < 1$  relies on 10 cm wide drift tubes [3], while 1 cm mini-drift tubes are used at  $1 < |\eta| < 2$  [4].

## III. DATA AND MONTE CARLO SAMPLES

The data sample used in the presented analysis was collected by the DØ detector at the Fermilab Tevatron  $p\bar{p}$  collider at a center-of-mass energy of 1.96 TeV between August 2002 and March 2004 and corresponds to an integrated luminosity of  $\mathcal{L} \approx 221 \text{ pb}^{-1}$ . In order to ensure that the data are described correctly by the Monte Carlo (MC), a well-known process is examined:  $Z \rightarrow \mu^+\mu^-$ . To obtain a proper MC normalization the  $Z \rightarrow \mu^+\mu^-$  MC is adjusted to the data in a mass range of 60-120 GeV.

All simulated processes for the supersymmetric signal and the Standard Model (SM) background are generated using PYTHIA 6.202 [5] and processed through the full detector simulation. The supersymmetric signal parameters have been generated for  $\tan\beta = 3$  and chargino masses in a range of 100-115 GeV. The total cross section  $\sigma \times BR(p\bar{p} \rightarrow \tilde{\chi}_1^\pm \tilde{\chi}_2^0 \rightarrow 3\ell)$  varies between 0.2 and 0.4 pb. A detailed description of the generated supersymmetric signal points is given in Table I. The expected background from Standard Model processes are  $Z/\gamma^* \rightarrow \mu^+\mu^-$  ( $Z/\gamma^* \rightarrow \tau^+\tau^-$ ),

TABLE I: Monte Carlo reference points for the supersymmetric signal. All masses are given in GeV.

Point	$\tan\beta$	$m_0$	$m_{1/2}$	$A_0$	$\text{sgn}(\mu)$	$m_{\tilde{\chi}_2^0}$	$m_{\tilde{\chi}_1^\pm}$	$m_{\tilde{\ell}_R}$	$m_{\tilde{\tau}_L}$	$m_{\tilde{\chi}_1^0}$	$\sigma \times BR$ [pb]	Generated Events
1	3	72	165	0	+	102	97	102	101	57	0.39	17500
2	3	76	170	0	+	106	101	106	105	59	0.32	25700
3	3	80	175	0	+	110	105	110	109	62	0.27	23900
4	3	84	180	0	+	114	110	114	113	64	0.21	25400
5	3	88	185	0	+	118	114	118	117	67	0.18	20000

$WZ \rightarrow \mu^+\nu\mu^-\mu^+$  and  $WW \rightarrow \mu^+\nu\mu^-\bar{\nu}$ . The background contribution from QCD production is determined from data.

TABLE II: Selection cuts applied in order to discriminate between signal and background

(1) Preselection	$p_T > 9.0$ GeV, $p_T > 5.0$ GeV muons must have at least 3 hits in the inner SMT DCA < 0.16 cm muons are isolated muons are from same vertex cosmic muons are removed
(2) Anti $Z \rightarrow \mu\mu$	$15 < M_{\mu\mu} < 50$ GeV
(3) selection of an isolated charged track	$p_T > 3.0$ GeV
(4) $\cancel{E}_T$	$\cancel{E}_T > 22.0$ GeV
(5) $\cancel{E}_T \times p_T$ of isolated charged track	$p_T \times \cancel{E}_T > 100.0$
(6) invariant mass	$M_{\mu_1, track} > 15.0$ GeV, $M_{\mu_2, track} > 12.0$ GeV
(7) $\Delta\phi_1$	$\Delta\phi(\cancel{E}_T, p_T^{\mu_1}) > 2.0$
(8) $\Delta\phi_2$	$\Delta\phi(\cancel{E}_T, p_T^{\mu_2}) > 1.5$
(9) leading muon $p_T^{\mu_1}$	$p_T^{\mu_1} > 15.0$ GeV

#### IV. EVENT SELECTION

The supersymmetric signal under examination requires events with two opposite sign muons, an additional charged lepton (muon, electron or tau) and missing transverse energy ( $\cancel{E}_T$ ) in the final state. The requirement of an additional charged lepton was replaced with the requirement of an isolated charged track. The main discriminants for signal and background are: two identified muons,  $\cancel{E}_T$ , an isolated charged track and the reconstructed invariant mass from the two identified muons. The large amount of missing energy in the signal processes is due to the  $\tilde{\chi}_1^0$  and the neutrino. The detailed selection flow is shown in Table II.

Events with two muons matched to a reconstructed track in the inner detector are selected. For good tracking quality a minimum number of at least three hits in the Silicon Microstrip Tracker (SMT) are required for each muon. The two leading  $p_T$  muons are required to have  $p_T > 9.0$  GeV,  $p_T > 5.0$  GeV and must fulfill the tracking isolation criterion ( $\Sigma_{track}^{\Delta R < 0.5} p_T < 2.5$  GeV,  $\Delta R = \sqrt{\eta^2 + \phi^2}$ , where  $\eta$  is the pseudo-rapidity and  $\phi$  the angle) and the calorimeter isolation criterion (energy deposited in the calorimeter cells  $\Sigma_{cells}^{0.1 < \Delta R < 0.4} E_T < 2.5$  GeV). Muons are reconstructed from the same primary vertex. In order to reduce cosmic background timing cuts are applied for selected muons and the distance of closest approach (DCA) of the reconstructed track with respect to the vertex is required to be smaller than 0.16 cm.

The reconstructed invariant mass  $M_{\mu\mu}$  (Figure 2a) and the missing transverse energy distribution (Figure 2b) for the selected events after preselection show the  $Z \rightarrow \mu^+\mu^-$ ,  $Z \rightarrow \tau^+\tau^-$ , Drell-Yan ( $Z/\gamma^* \rightarrow \mu^+\mu^-$ ,  $Z/\gamma^* \rightarrow \tau^+\tau^-$ ),  $WZ \rightarrow \mu^+\nu\mu^-\mu^+$ ,  $WW \rightarrow \mu^+\nu\mu^-\bar{\nu}$  and  $t\bar{t} \rightarrow b\mu\nu b\mu\nu$  backgrounds. The signal distribution shown by the magenta line in each figure corresponds to Point 2 of Table I.

In order to reduce the  $Z \rightarrow \mu^+\mu^-$  events, the reconstructed invariant mass is required to be  $15.0 < M_{\mu\mu} < 50.0$  GeV. This cut is applied for both, same sign and opposite sign dimuon events.

To further reduce the SM background the additional charged track is selected. This track must have a  $p_T$  larger than 3.0 GeV, must fulfill the tracking isolation criterion ( $\Sigma_{track}^{0.1 < \Delta R < 0.4} p_T < 1.0$  GeV), the pseudo-rapidity is  $|\eta| < 2.0$ , and the  $\chi^2/NDF$  of the track fit must be less than 4.0. In addition the track must be well separated from the selected muons in  $\Delta R$  by more than 0.4 and must be from the same primary vertex as the selected muons. The  $p_T$  distribution is shown in Figure 2c.

The missing transverse energy after all previous cuts is shown in Figure 2d. Only events with  $\cancel{E}_T > 22.0$  GeV are selected.

The reconstructed invariant mass of the selected leading  $p_T$  muon and the isolated charged track is shown in Figure 3. A cut is applied to the invariant masses (leading  $p_T$  muon and isolated charged track  $M_{\mu_1, track} > 15.0$  GeV and next-to leading  $p_T$  muon and isolated charged track  $M_{\mu_2, track} > 12.0$  GeV). A further cut is applied for the angle between the selected muons and  $\cancel{E}_T$ . Only events with  $\Delta\phi(\cancel{E}_T, p_T^{\mu_1}) > 2.0$  and  $\Delta\phi(\cancel{E}_T, p_T^{\mu_2}) > 1.5$  are selected. Finally the last cut is applied to the transverse momentum for the leading  $p_T$  muon  $p_T^{\mu_1} > 15.0$  GeV. This cut reduces the QCD background further.

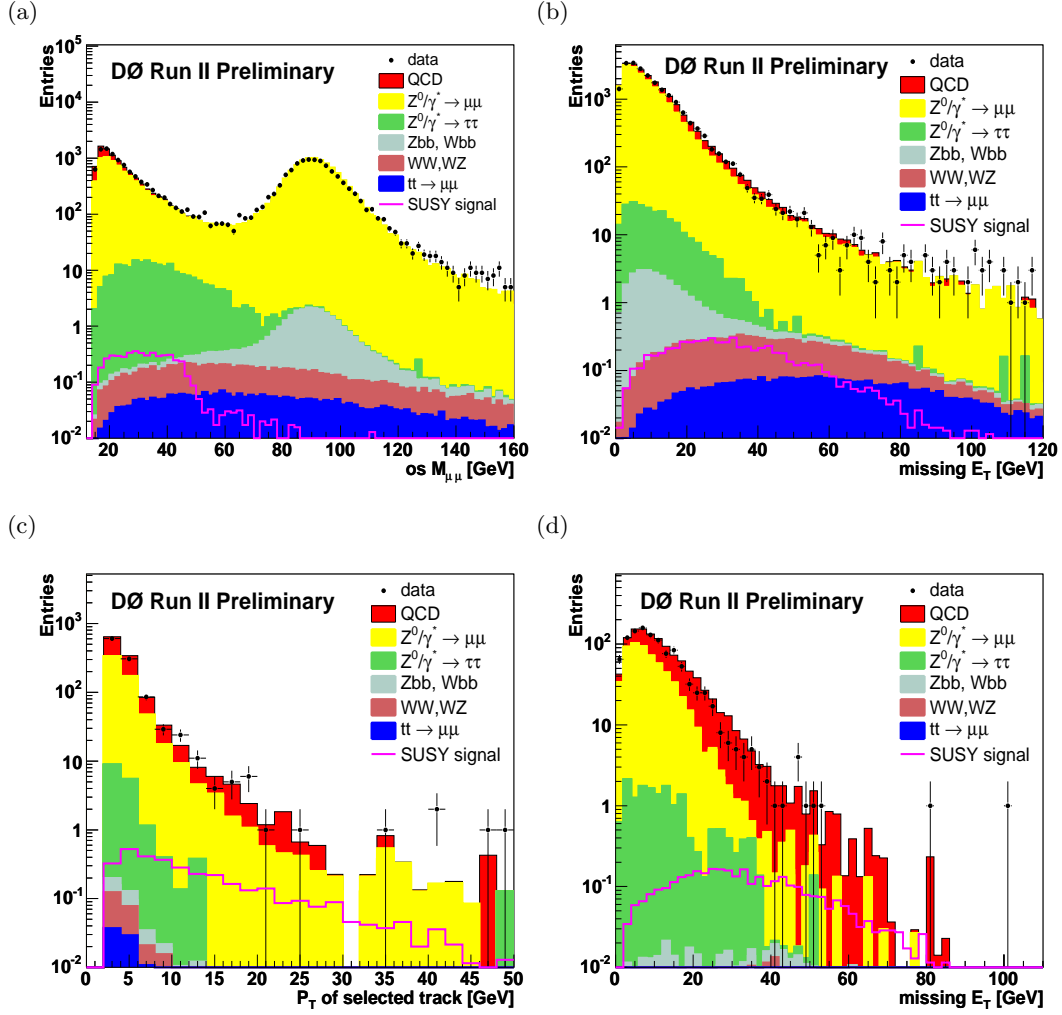


FIG. 2: (a) Invariant dimuon mass for opposite sign muons ( $os M_{\mu\mu}$ ) after preselection, (b) missing transverse energy after preselection, (c) transverse momentum of the selected charged track (after cut (1)-(2) from Table II), (d) missing transverse energy (after cut (1)-(3) from Table II). The magenta line in each figure shows the distribution of the supersymmetric signal (Point 2 from Table I).

## V. RESULTS

The number of data events and expected background events (from SM processes) are shown in Table III. The events in SUSY Monte Carlo after each cut are shown in Table IV.

After all cuts one candidate is selected in the data, while the number of events from the expected MC background is  $1.83 \pm 0.45$  mostly arising from Drell-Yan  $Z/\gamma^* \rightarrow \mu^+\mu^-$  and  $Z \rightarrow \mu^+\mu^-$  processes. The error on the expected background is dominated by the limited  $Z/\gamma^* \rightarrow \mu^+\mu^-$  statistics.

The number of signal events is in the range of 0.7 to 1.3 events.

The systematic errors arise from several sources. A large contribution comes from the error on the  $Z \rightarrow \mu^+\mu^-$  cross section. The spectra for the reconstructed  $p_T$  of the  $Z/\gamma^* \rightarrow \mu^+\mu^-$  was reweighted in order to describe the data correctly. This results in a systematic error on the  $Z/\gamma^* \rightarrow \mu^+\mu^-$ . More systematic errors arise from the correction of the MC ( $p_T$  smearing).

The systematic error for the supersymmetric signal events is due to the error on the  $Z \rightarrow \mu^+\mu^-$  cross section and the  $p_T$  smearing of the Monte Carlo.

## VI. CONCLUSIONS

A search for supersymmetry for the trilepton channel has been performed. Final states with two muons and an additional isolated charged track (the requirement of an additional lepton was replaced with the requirement of

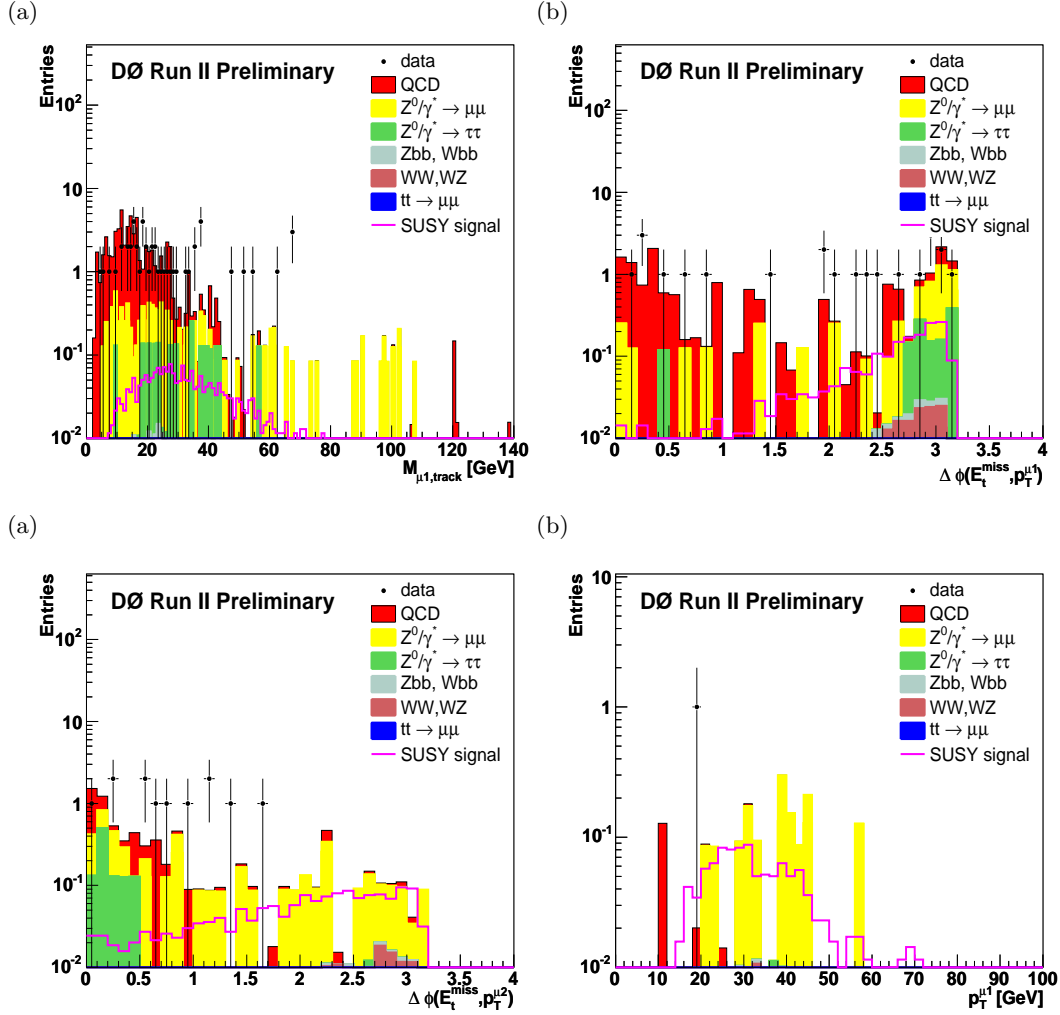


FIG. 3: (a) Invariant mass of the leading  $p_T$  muon ( $p_T^{\mu 1}$ ) and isolated charged track (after cut (1)-(5) from Table II), (b) angle distribution between  $p_T^{\mu 1}$  and the  $E_T$  (after cut (1)-(6) from Table II), (c) angle distribution between the next-to-leading  $p_T^{\mu 2}$  and the  $E_T$  (after cut (1)-(8) from Table II), (d)  $p_T$  distribution of the leading muon. The magenta line in each figure shows the distribution of the supersymmetric signal (Point 2 from Table I).

an isolated charged track) arising from the subsequent decay of the chargino  $\tilde{\chi}_1^\pm$  and the neutralino  $\tilde{\chi}_2^0$  have been analyzed with data corresponding to an integrated luminosity of  $\mathcal{L} \approx 221 \text{ pb}^{-1}$ . The analysis is not yet sensitive for the mSUGRA points in the mass range beyond the LEP chargino limits. A combination with the  $e+\mu$  and the  $e+e$  topologies will improve the sensitivity.

### Acknowledgments

We thank the staffs at Fermilab and collaborating institutions, and acknowledge support from the Department of Energy and National Science Foundation (USA), Commissariat à l’Energie Atomique and CNRS/Institut National de Physique Nucléaire et de Physique des Particules (France), Ministry of Education and Science, Agency for Atomic Energy and RF President Grants Program (Russia), CAPES, CNPq, FAPERJ, FAPESP and FUNDUNESP (Brazil), Departments of Atomic Energy and Science and Technology (India), Colciencias (Colombia), CONACyT (Mexico), KRF (Korea), CONICET and UBACyT (Argentina), The Foundation for Fundamental Research on Matter (The Netherlands), PPARC (United Kingdom), Ministry of Education (Czech Republic), Natural Sciences and Engineering Research Council and WestGrid Project (Canada), BMBF (Germany), A.P. Sloan Foundation, Civilian Research and Development Foundation, Research Corporation, Texas Advanced Research Program, and the Alexander von

TABLE III: Number of events from data and expected Monte Carlo background after each cut. The errors are statistical except for the Sum of MC background, where the systematic errors are also given.

	Data	Sum	$Z \rightarrow \mu\mu$	$Z \rightarrow \tau\tau$	QCD
(1) ID+isol	21221	21107.91 $\pm$ 239.30 $\pm$ 204.82	17933.80 $\pm$ 45.33	224.03 $\pm$ 5.24	2913.91 $\pm$ 234.91
(2) Anti-Z	10063	10022.96 $\pm$ 236.82 $\pm$ 223.56	6929.72 $\pm$ 33.75	182.62 $\pm$ 4.74	2906.94 $\pm$ 234.35
(3) 3rd track	1087	1197.00 $\pm$ 46.56 $\pm$ 75.62	631.53 $\pm$ 9.37	16.95 $\pm$ 1.45	547.99 $\pm$ 45.59
(4) $\cancel{E}_T$	82	101.23 $\pm$ 8.23 $\pm$ 22.25	16.69 $\pm$ 1.37	2.90 $\pm$ 0.60	81.27 $\pm$ 8.09
(5) $p_T \times \cancel{E}_T$	50	65.64 $\pm$ 5.86 $\pm$ 15.19	9.29 $\pm$ 1.00	2.0 $\pm$ 0.50	53.99 $\pm$ 5.74
(6) invmass	22	18.13 $\pm$ 2.28 $\pm$ 3.07	4.60 $\pm$ 0.68	1.26 $\pm$ 0.40	12.04 $\pm$ 2.14
(7) $\Delta\phi_1$	12	7.89 $\pm$ 1.13 $\pm$ 0.63	3.61 $\pm$ 0.58	1.26 $\pm$ 0.40	2.83 $\pm$ 0.88
(8) $\Delta\phi_2$	1	1.97 $\pm$ 0.43 $\pm$ 0.21	1.34 $\pm$ 0.36	0.25 $\pm$ 0.18	0.22 $\pm$ 0.14
(9) $p_T^{\mu_1}$	1	1.83 $\pm$ 0.40 $\pm$ 0.21	1.34 $\pm$ 0.36	0.25 $\pm$ 0.18	0.08 $\pm$ 0.01

	Wbb	Zbb	WZ	WW	$t\bar{t}$
(1) ID+isol	0.46 $\pm$ 0.02	25.11 $\pm$ 0.14	0.47 $\pm$ 0.01	6.79 $\pm$ 0.07	3.36 $\pm$ 0.03
(2) Anti-Z	0.41 $\pm$ 0.02	0.51 $\pm$ 0.02	0.06 $\pm$ 0.00	1.95 $\pm$ 0.04	0.78 $\pm$ 0.01
(3) 3rd track	0.06 $\pm$ 0.01	0.14 $\pm$ 0.01	0.03 $\pm$ 0.00	0.16 $\pm$ 0.01	0.13 $\pm$ 0.01
(4) $\cancel{E}_T$	0.05 $\pm$ 0.01	0.04 $\pm$ 0.01	0.03 $\pm$ 0.00	0.14 $\pm$ 0.01	0.12 $\pm$ 0.01
(5) $p_T \times \cancel{E}_T$	0.04 $\pm$ 0.01	0.04 $\pm$ 0.01	0.03 $\pm$ 0.00	0.12 $\pm$ 0.01	0.10 $\pm$ 0.00
(6) invmass	0.01 $\pm$ 0.00	0.03 $\pm$ 0.00	0.02 $\pm$ 0.00	0.08 $\pm$ 0.01	0.09 $\pm$ 0.00
(7) $\Delta\phi_1$	0.01 $\pm$ 0.00	0.02 $\pm$ 0.00	0.02 $\pm$ 0.00	0.08 $\pm$ 0.01	0.05 $\pm$ 0.00
(8) $\Delta\phi_2$	0.01 $\pm$ 0.00	0.01 $\pm$ 0.00	0.02 $\pm$ 0.00	0.07 $\pm$ 0.01	0.05 $\pm$ 0.00
(9) $p_T^{\mu_1}$	0.01 $\pm$ 0.00	0.01 $\pm$ 0.00	0.02 $\pm$ 0.00	0.07 $\pm$ 0.01	0.05 $\pm$ 0.00

TABLE IV: Number of events for different SUSY points after each cut. The errors are statistical and systematic.

Cut	Point 1	Point 2	Point 3	Point 4	Point 5
(1) ID+isol	7.55 $\pm$ 0.14 $\pm$ 0.84	6.34 $\pm$ 0.10 $\pm$ 0.70	5.41 $\pm$ 0.08 $\pm$ 0.60	4.25 $\pm$ 0.07 $\pm$ 0.47	3.70 $\pm$ 0.06 $\pm$ 0.41
(2) Anti-Z	6.32 $\pm$ 0.13 $\pm$ 0.70	5.28 $\pm$ 0.09 $\pm$ 0.59	4.46 $\pm$ 0.08 $\pm$ 0.49	3.43 $\pm$ 0.06 $\pm$ 0.38	2.91 $\pm$ 0.05 $\pm$ 0.32
(3) 3rd track	4.07 $\pm$ 0.10 $\pm$ 0.45	3.51 $\pm$ 0.07 $\pm$ 0.38	2.94 $\pm$ 0.06 $\pm$ 0.33	2.21 $\pm$ 0.05 $\pm$ 0.25	1.90 $\pm$ 0.04 $\pm$ 0.21
(4) $\cancel{E}_T$	2.93 $\pm$ 0.09 $\pm$ 0.32	2.53 $\pm$ 0.06 $\pm$ 0.28	2.20 $\pm$ 0.05 $\pm$ 0.24	1.67 $\pm$ 0.04 $\pm$ 0.19	1.47 $\pm$ 0.04 $\pm$ 0.17
(5) $p_T \times \cancel{E}_T$	2.86 $\pm$ 0.08 $\pm$ 0.32	2.47 $\pm$ 0.06 $\pm$ 0.28	2.16 $\pm$ 0.05 $\pm$ 0.23	1.64 $\pm$ 0.04 $\pm$ 0.18	1.43 $\pm$ 0.04 $\pm$ 0.16
(6) invmass	2.18 $\pm$ 0.07 $\pm$ 0.24	1.91 $\pm$ 0.05 $\pm$ 0.22	1.72 $\pm$ 0.05 $\pm$ 0.19	1.28 $\pm$ 0.03 $\pm$ 0.14	1.16 $\pm$ 0.03 $\pm$ 0.13
(7) $\Delta\phi_1$	1.81 $\pm$ 0.07 $\pm$ 0.20	1.56 $\pm$ 0.05 $\pm$ 0.18	1.42 $\pm$ 0.04 $\pm$ 0.16	1.08 $\pm$ 0.03 $\pm$ 0.12	0.96 $\pm$ 0.03 $\pm$ 0.11
(8) $\Delta\phi_2$	1.32 $\pm$ 0.06 $\pm$ 0.15	1.14 $\pm$ 0.04 $\pm$ 0.13	1.07 $\pm$ 0.04 $\pm$ 0.12	0.82 $\pm$ 0.03 $\pm$ 0.09	0.72 $\pm$ 0.03 $\pm$ 0.08
(9) $p_T^{\mu_1}$	1.28 $\pm$ 0.06 $\pm$ 0.14	1.12 $\pm$ 0.04 $\pm$ 0.12	1.06 $\pm$ 0.04 $\pm$ 0.12	0.80 $\pm$ 0.03 $\pm$ 0.09	0.70 $\pm$ 0.03 $\pm$ 0.07

Humboldt Foundation.

- 
- [1] S. Martin,  
*A Supersymmetry Primer* hep-ph/9709356
  - [2] The DØ Collaboration, S.Abachi et al.  
*The DØ Upgrade: The Detector and its Physics.*  
 Fermilab Pub-96/357-E (1996)
  - [3] S. Abachi, et al.  
*The DØ Detector* Nucl.Instrum.Meth.A338:185-253,1994
  - [4] S. Abachi, et al.  
 Forward Muon System for the DØ Detector Upgrade Nucl.Instrum.Meth.A419:660-666,1998
  - [5] T. Sjöstrand, Comp. Phys. Comm. 82 (1994) 74.